

Spin Glass Behavior of New Perovskites $\text{Ba}_2\text{In}_{2-x}\text{Co}_x\text{O}_5$ ($0.5 \leq x \leq 1.70$)

A. D. Lozano Gorrín,* P. Núñez,* M. A. López de la Torre,† J. Romero de Paz,‡
and R. Sáez Puche†¹

*Departamento de Química Inorgánica, Universidad de La Laguna, 38206-La Laguna, Tenerife, Spain; †Departamento de Física Aplicada, Universidad de Castilla-La Mancha, Campus Universitario, 13071 Ciudad Real, Spain; and ‡Departamento de Química Inorgánica, Facultad de Ciencias Químicas, Universidad Complutense Madrid, 28040 Madrid, Spain

Received October 4, 2001; in revised form December 26, 2002; accepted January 18, 2002; published online March 22, 2002

New oxides of general formula $\text{Ba}_2\text{In}_{2-x}\text{Co}_x\text{O}_5$ ($0.5 \leq x \leq 1.70$) have been synthesized as polycrystalline materials and fully characterized by means of X-rays. They are all isostructural and crystallize in a perovskite-type structure, showing cubic symmetry, space group $Pm\bar{3}m$. The magnetic properties of these oxides have been studied by χ_{ac} and χ_{dc} measurements as a function of magnetic field and temperature. In the case of $x = 0.5$ ($\text{BaIn}_{1.50}\text{Co}_{0.5}\text{O}_5$) the sample remains paramagnetic from 200 to 2 K. However, the magnetic behavior of the oxides $\text{Ba}_2\text{In}_{2-x}\text{Co}_x\text{O}_5$ ($0.70 \leq x \leq 1.70$) is rather different: χ_{dc} shows broad maxima which are shifted with the x cobalt content. Below this temperature a strong irreversibility between the zero-field-cooled (ZFC) and field-cooled (FC) curves has been detected, more pronounced as the cobalt content is higher. χ_{ac} measurements also show all the common features of spin glasses, fully confirmed from the analysis of the non linear part of the χ_{dc} . © 2002 Elsevier Science (USA)

Key Words: In–Co perovskites; spin-glass; nonlinear magnetic susceptibility.

INTRODUCTION

Many transition oxides show the very versatile structure of perovskite. The rich variety of physical properties such as high-temperature superconductivity, giant magnetoresistance, and spin glasses observed in these compounds makes them very attractive for both academic and technological purposes.

Compounds belonging to the $\text{BaO–In}_2\text{O}_3$ ternary system have been the concern of different studies, including single-crystal X-ray diffraction analysis, which show that most of them are derived from the cubic perovskite structure (1–5). $\text{Ba}_3\text{In}_2\text{O}_6$ (6) and $\text{Ba}_4\text{In}_2\text{O}_7$ (7) can be described as layers of InO_5 square pyramids. The existence of $\text{Ba}_2\text{In}_2\text{O}_5$ crystallizing in an orthorhombic-perovskite subcell with para-

eters $a_o = 6.111(1)$ Å, $b_o = 5.992(1)$ Å, $c_o = 4.204(2)$ Å has been reported (4). Even though a related phase, $\text{BaInO}_{2.5}$, which was prepared at 1400°C (6), has also been described as a cubic perovskite ($a = 4.219(2)$ Å), such a structure was not observed at temperatures up to 1300°C (1). Several authors (1, 2) have found that $\text{Ba}_2\text{In}_2\text{O}_5$, as well as $\text{Sr}_2\text{In}_2\text{O}_5$ (8), is isotypic with $\text{Ca}_2\text{FeAlO}_5$ (brownmillerite) (9), where the In(III) ions are located in both tetrahedral and octahedral coordination.

On the other hand, the solid solutions $\text{Ba}_2M_{2-x}\text{Cu}_x\text{O}_{4+\delta}$, $M = \text{In, Sc, Lu}$, have also been synthesized and characterized, leading to a double perovskite structure (2, 10). More recently, we have prepared the compound $\text{Ba}_2\text{ScCoO}_5$, which has been described as a cubic oxygen-deficient single perovskite with the B-sites randomly occupied by Sc and Co atoms (11).

Magnetic materials with triangle-based lattice with frustrate magnetic interactions have been the subject of many studies in the past 20 years (12–14). Different structural types have served as models to investigate their geometrical frustration. More recently, magnetic frustration giving rise to spin-glass behavior has been reported for perovskite oxides of general formula $A_2BB'O_6$, where the B and B' ions are settled with either random or ordered arrangement (15).

Recently, different cobalt oxide perovskites having a cubic structure have been reported, where the B site accommodates the random occupation of the Co and different diamagnetic cations. This produces a kind of magnetic dilution of the cobalt in the B sublattice that yields a spin-glass-like behavior transition at low temperatures (16, 17).

Cobalt is well known to exhibit three different spin configurations for the Co^{3+} ion in octahedral environment, denoted as high-spin (HS; $S = 2$), intermediate-spin (IS; $S = 1$), and low-spin (LS; $S = 0$). These spin states are a function of the temperature and many studies have been reported concerning the spin transition in LaCoO_3 , but

¹To whom correspondence should be addressed. Fax: 33913944352. E-mail: RSP92@quim.ucm.es.

recent reports (18, 19) establish a consensus upon these transitions that take place in LaCoO_3 following the sequence $\text{LS} \rightarrow \text{IS} \rightarrow \text{HS}$ with increasing temperature. The coexistence of these IS and HS states of Co^{3+} in the case of the perovskite $\text{Ba}_2\text{CoNbO}_6$ has been stated to be the origin of the magnetic frustration yielding the spin-glass behavior displayed by this material (16).

The aim of our work is to prepare perovskites of the type $\text{Ba}_2\text{In}_{2-x}\text{Co}_x\text{O}_5$, for x values going to 0.5 to 1.7, which have been characterized and to assess the influence of the cobalt content along this solid solution on the magnetic properties.

EXPERIMENTAL

$\text{BaIn}_{2-x}\text{Co}_x\text{O}_5$ ($0.5 \leq x \leq 1.70$) samples were prepared by solid state reactions from stoichiometric amounts of In_2O_3 (99.9%), $\text{Co}(\text{Ac})_2 \cdot 4\text{H}_2\text{O}$ (99%), and BaCO_3 . The mixtures were heated in air overnight for carbonate decomposition at 850°C and then for 5 days at 1050°C with several intervening regrinding to obtain the oxides as polycrystalline materials. The samples were cooled in the furnace from the reaction temperature to room temperature.

Powder X-ray diffraction at room temperature was carried out in a Philips X'Pert diffractometer using the $\text{CuK}\alpha$ radiation, in the angular range $10^\circ < 2\theta < 120^\circ$, by step scanning in increments of 0.02° and a counting time of 5s per step. The data were analyzed using the Rietveld method (20) using the FULLPROF program (21). A pseudo-Voigt function was used to describe the peak shape and a polynomial function with five refinable coefficients for the background.

χ_{dc} and χ_{ac} magnetic susceptibility measurements were performed using a SQUID XL magnetometer from Quantum Design in the temperature range from 2 to 300 K. Measurements of susceptibility as a function of external magnetic field up to 1 kOe were performed. Susceptibility was measured using field-cooled (FC) and zero-field-cooled (ZFC) processes.

RESULTS AND DISCUSSION

Structural Characterization

X-ray powder diffraction patterns reveal that all the samples have been obtained as pure phases. The patterns have been indexed using the aristotype perovskite as a model, with cubic space group $Pm\bar{3}m$ (No. 221). The X-ray diffraction pattern refined by the Rietveld method for the sample $\text{Ba}_2\text{In}_{0.5}\text{Co}_{1.5}\text{O}_5$ is shown in Fig. 1. Cell parameters and reliability factors are summarized in Table 1.

It should be emphasized that while the studied phases $\text{Ba}_2\text{In}_{2-x}\text{Co}_x\text{O}_5$ show a cubic perovskite structure, that is not the case for the limit compounds. At one end ($x=0$) is found the brownmillerite structure ($\text{Ba}_2\text{In}_2\text{O}_5$: $a=6.095(1)$ Å, $b=16.7112(1)$ Å, $c=5.9601$ Å, $Ibm2$ (2)), and at the other end ($x=1$) is found the hexagonal perovskite (BaCoO_3 : $a=5.645(3)$ Å, $c=4.752$ Å, $\gamma=120^\circ$, $P6_3/mmc$ (22, 23)).

In the brownmillerite structure, $\text{Ba}_2\text{In}_2\text{O}_5$, which derives from the perovskite structure, there are alternating layers of In (III) in octahedral and tetrahedral coordination sites. The cubic symmetry is indicative of the existence of a disorder distribution of the cations in the B positions of the

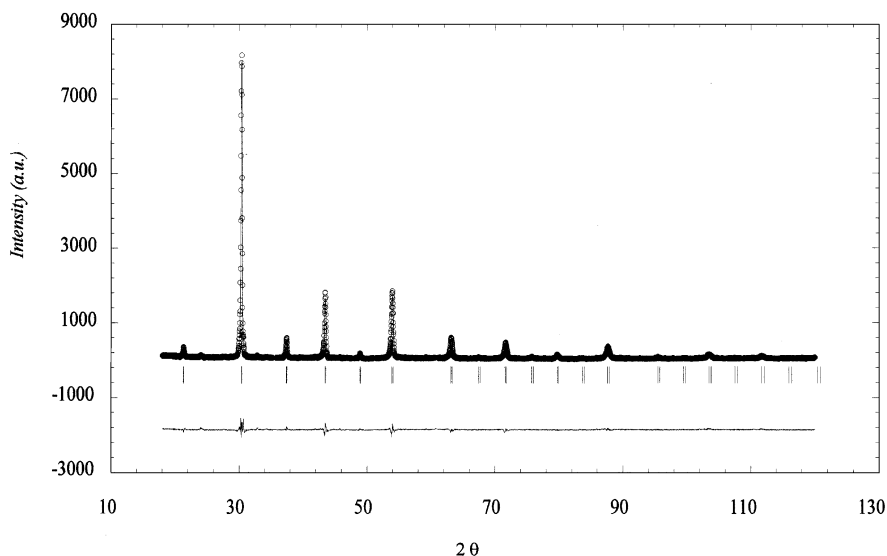


FIG. 1. Observed (dots) and calculated (solid line) X-ray diffraction patterns for $\text{Ba}_2\text{InCoO}_5$ oxide. The lower part of the figure shows the difference between observed and calculated plots, and the vertical marks are the allowed reflections for this perovskite oxide.

TABLE 1
Cell Parameters and Reliability Factors Obtained from the Rietveld Refinement

Compound	a (Å)	V (Å ³)	χ^2	R_p	R_{wp}	R_{exp}	R_{Bragg}
Ba ₂ In _{1.5} Co _{0.5} O ₅	4.2277(2)	75.563	5.02	13.2	18.1	8.07	10.1
Ba ₂ In _{1.3} Co _{0.7} O ₅	4.1751(1)	72.780	3.58	16.5	21.0	11.1	8.17
Ba ₂ InCoO ₅	4.1623(2)	72.109	3.67	12.4	15.3	8.01	8.41
Ba ₂ In _{0.3} Co _{1.7} O ₅	4.1191(2)	69.890	2.28	9.93	13.1	8.65	5.91

Number of refined parameters: 17; Reflection number: 44.

perovskite and a random location of oxygen vacancies in the structure. Considering cobalt in the trivalent oxidation state for the title compounds, the average coordination number for both indium and cobalt ions should be 5. In the case of the brownmillerite structure the coordination number is averaged also to 5, as a result of the tetrahedral and octahedral geometries for indium atoms. In our case, this average coordination number of 5 leads to a large number of anionic vacancies (one over six) that introduces a strong distortion in the octahedra. Even though the indium atoms show a preference for being located in tetrahedral sites, they should be in a disordered distribution, as a global cubic symmetry is observed from the X-ray diffraction patterns.

The decrease in the cell parameter observed (see Table 1) when the cobalt content increases can be explained by the replacement of Co³⁺ ($r_{HS}^6 = 0.75$, $r_{LS}^6 = 0.68$ Å) by the larger In³⁺ ($r^6 = 0.94$ Å) (15).

Magnetic Properties

Figure 2 shows the temperature dependence of the magnetic susceptibility for the oxide of composition Ba₂In_{1.5}Co_{0.5}O₅ as measured in an applied magnetic field

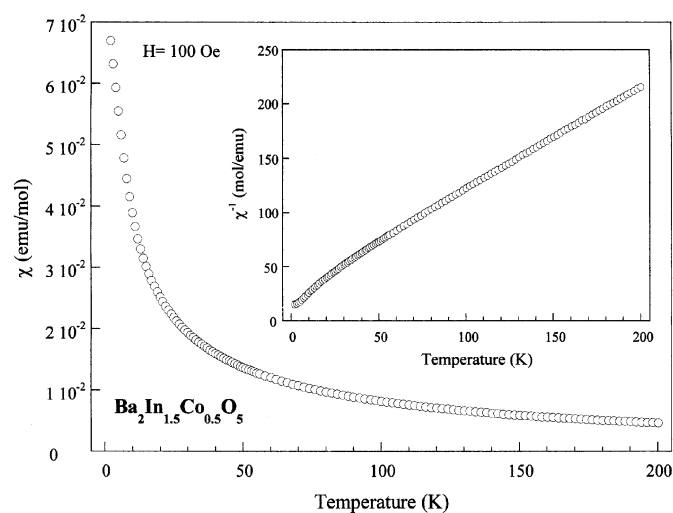


FIG. 2. Temperature dependence of the molar magnetic susceptibility for Ba₂In_{1.5}Co_{0.5}O₅ oxide. The inset is the χ^{-1} vs T plot.

of 100 Oe. The magnetic susceptibility follows a Curie–Weiss law (Fig. 2, inset) in the whole range of temperature 200–2 K and the calculated magnetic moment of 4.03 BM is indicative of the coexistence of Co³⁺ in the different states of spin mentioned above. According to the Hund’s rules the ground state of the Co³⁺ free ion (3d⁶) has a $S = 2$ spin value corresponding to the high-spin configuration. But in octahedral coordination can adopt both high- ($t_{2g}^4 e_g^2$, $S = 2$) and low- ($t_{2g}^6 e_g^0$, $S = 0$) spin configurations. The high-spin state (HS), which yields ${}^5T_{2g}$ as ground term, occurs in weak octahedral ligand fields, as it is found in fluorides, and yields an important orbital contribution to the magnetic moment (24). The low spin (LS) state is found in strong ligand fields, has ${}^1A_{1g}$ as ground term, and will yield diamagnetic susceptibility values. Oxygen is in the middle of the spectrochemical series and shows an intermediate value of the crystal field Dq . In fact, in oxides containing (CoO₆) octahedra, the energy gap between these two states is only 0.08 eV and consequently the transition from the less energetic low-spin (LS) Co³⁺ (A_1) to the high-spin (HS) Co³⁺ (5T_2) is relatively easy (25). Additionally, an intermediate spin (IS) state ($t_{2g}^5 e_g^1$) yielding a ${}^3T_{1g}$ (3H) term has been proposed as the ground state in lower symmetries such as axially distorted octahedra (26), which in our case could be induced by the anionic vacancies.

As we indicated above, the obtained magnetic moment of 4.03 BM is intermediate between the theoretical value for the HS state, with a spin-only contribution of 4.9 BM, and the IS state of 2.8 BM. The estimated Co³⁺ in the HS state is about 83% of the total amount of Co³⁺, while only the remaining 17% will correspond to the IS state. This particular paramagnetic behavior can be explained by taking into account the random distribution of the paramagnetic Co³⁺ into the diamagnetic In³⁺ matrix. It can be also stated that the LS state is not attained even down to 2 K as in the case of the Sr₂CoSbO₆ (17) very recently reported and contrary to the classic LaCoO₃ (27).

The increase of the cobalt content leads to important changes in the magnetic properties. It can be observed that the magnetic susceptibility for Ba₂In_{1.30}Co_{0.70}O₅, Ba₂InCoO₅, and Ba₂In_{0.30}Co_{1.70}O₅, Figs. 3–5, follow a Curie–Weiss behavior in the temperature range 300–100 K. The magnetic moments take values from 4.28 to 3.04 BM, while the Weiss constants are negative in all cases that could

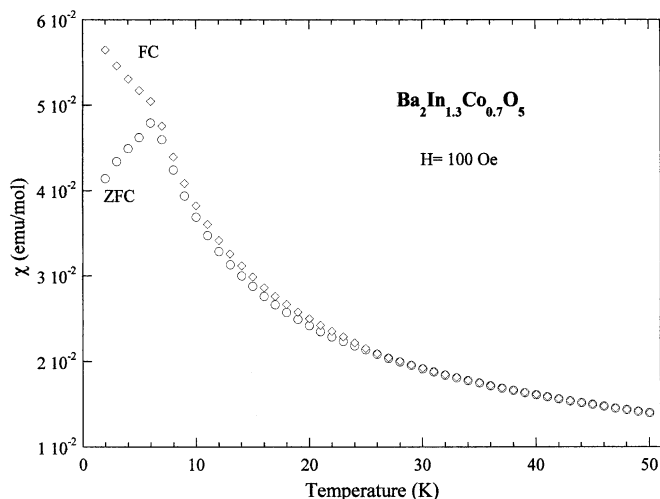


FIG. 3. Thermal variation of the magnetic susceptibility at 100 Oe in zero-field-cooled (ZFC) and field-cooled (FC) measurements for $\text{Ba}_2\text{In}_{1.3}\text{Co}_{0.7}\text{O}_5$.

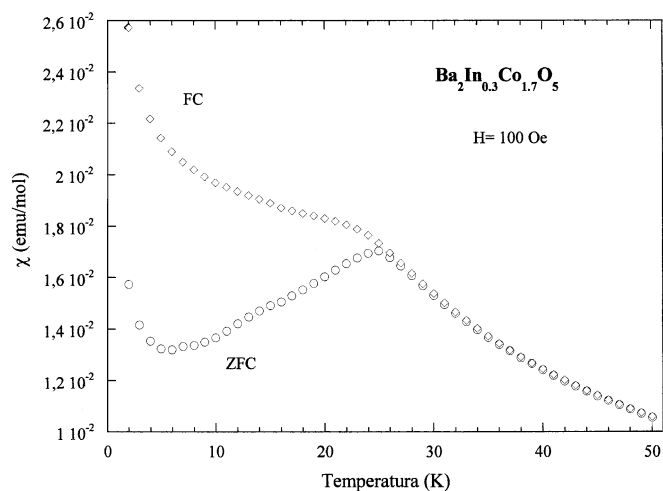


FIG. 5. Thermal variation of the magnetic susceptibility at 100 Oe in zero-field-cooling (ZFC) and field-cooling (FC) measurements for $\text{Ba}_2\text{In}_{0.3}\text{Co}_{1.7}\text{O}_5$.

indicate the existence of antiferromagnetic correlations of the Co^{3+} magnetic moments below the maximum which appears in all these samples. The obtained magnetic moments, Table 2, are indicative of the coexistence of Co^{3+} in HS and IS states of spin. Magnetic interactions between IS Co^{3+} ions ($t_{2g}^5 e_g^1$) are expected to be ferromagnetic as predicted by Goodenough's rule, since the interactions between HS Co^{3+} ($t_{2g}^4 e_g^2$) are antiferromagnetic (28). Thus, the competition between ferro and antiferromagnetic interactions leads to spin-glass behavior as a result of the magnetic frustration.

The differences between the FC and ZFC magnetization observed below the maximum found in the plots already

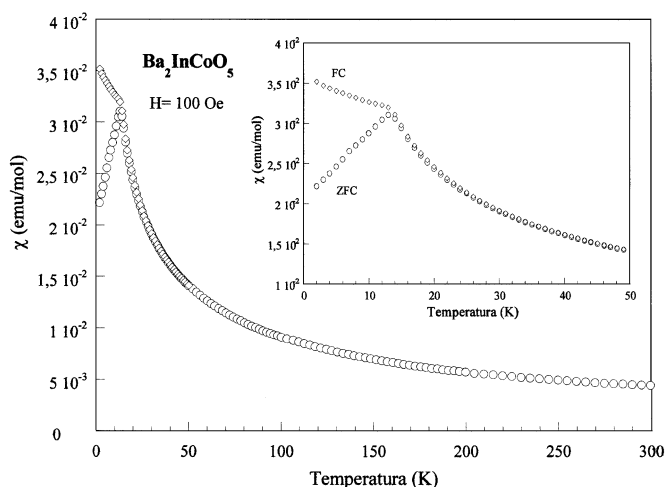


FIG. 4. Thermal variation of the magnetic susceptibility at 100 Oe in zero-field-cooling (ZFC) and field-cooling (FC) measurements for $\text{Ba}_2\text{InCoO}_5$.

mentioned could be assigned to the spin-glass behavior at these low temperatures. As in the case of canonical spin-glass materials, the transition temperature T_g increases with increased paramagnetic ions content, taking the value of 10 K for the $\text{Ba}_2\text{In}_{1.3}\text{Co}_{0.7}\text{O}_5$ and 30 K for the more concentrated sample $\text{Ba}_2\text{In}_{0.3}\text{Co}_{1.7}\text{O}_5$. In the case of $\text{Ba}_2\text{InCoO}_5$, with an intermediate composition, T_g takes the value of 20 K.

Figure 6 shows the ZFC and FC curves measured at different magnetic field strengths. It can be observed that the irreversibility between FC and ZFC curves is field dependent and the T_g value decrease gradually with the increase of the magnetic field, see Fig. 6, even at 5 T the transition is not completely suppressed. This behavior is usually found in spin-glass systems (29). However, these features alone are still ambiguous and they could also be explained within the superparamagnetism theory, where the maxima found in the susceptibility would indicate an accordingly a narrow size distribution of the magnetic clusters.

In order to gain deeper insight in the spin-glass behavior of these oxides, χ_{ac} measurements have been performed as

TABLE 2
Weiss Constant (θ), Magnetic Moment (μ), and Temperature at Which the Susceptibility Takes the Maximum Value ($T_{\chi_{\max}}$) Obtained for the Different $\text{Ba}_2\text{In}_{2-x}\text{Co}_x\text{O}_5$ Oxides

Compound	$\theta(K)$	$\mu(\mu_B)$	$T_{\chi_{\max}}(K)$
$\text{Ba}_2\text{In}_{1.5}\text{Co}_{0.5}\text{O}_5$	-22	4.03	—
$\text{Ba}_2\text{In}_{1.3}\text{Co}_{0.7}\text{O}_5$	-66	4.28	6
$\text{Ba}_2\text{InCoO}_5$	-52	3.33	12
$\text{Ba}_2\text{In}_{0.3}\text{Co}_{1.7}\text{O}_5$	-17	3.04	25

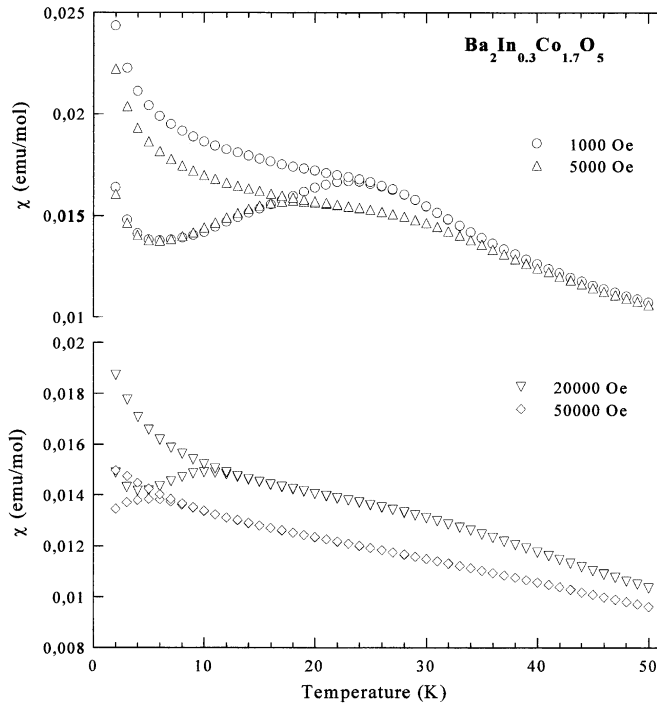


FIG. 6. Variation of the magnetic susceptibility at different magnetic fields in zero-field-cooling (ZFC) and field-cooling (FC) measurements for $\text{Ba}_2\text{In}_{0.3}\text{Co}_{1.7}\text{O}_5$.

a function of temperature at different frequencies and magnetic fields.

It has been also observed that the real part of the susceptibility χ' exhibits a maximum at 16 K which depends very weakly on the frequency of the ac field, as described in the literature for canonical spin glasses (29). This maximum is also affected by the application of relatively low dc fields and it smears out and shifts downwards, Fig. 7, as in the case of the isostructural $\text{Ba}_2\text{ScCoO}_5$ (11). The field dependence of T_g follows the so-called Almeida–Thouless (AT) law ($T_g \propto H^{2/3}$), this effect has also been demonstrated as characteristic encountered in spin-glasses (30). The observation of this set of phenomena has been often taken in the literature as sufficient to confirm the presence of a spin-glass system. However, it is worth noting that all the commented dynamical features can still be explained in terms of phenomenological model (31) derived from the Néel Theory of superparamagnetism (32).

In order to confirm the spin-glass behavior in these $\text{Ba}_2\text{In}_{2-x}\text{Co}_x\text{O}_5$ oxides, we have analysed the temperature dependence of the non-linear susceptibility (χ_{nl}) according to the Sherrington–Kirkpatrick mean-field model (33). The nonlinear coefficients of the magnetization were obtained as follows. M was developed in terms of $\chi_0 H$ instead of H , to avoid an overestimation of the nonlinear contribution to the susceptibility due to deviations from the Curie–Weiss

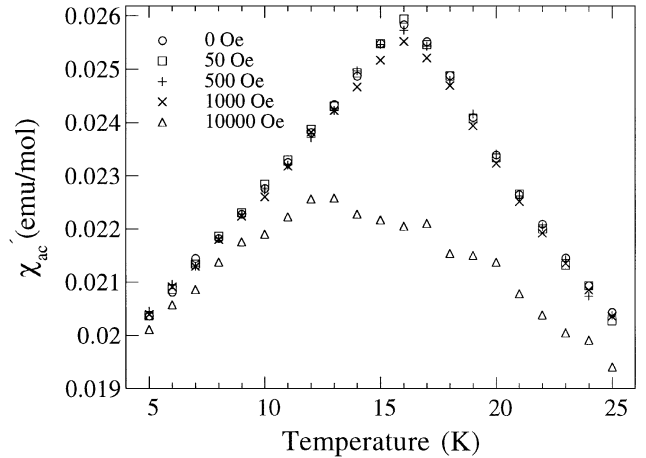


FIG. 7. Thermal dependence of the χ'_{ac} for different dc magnetic fields.

behavior at temperatures slightly above T_f (usually up to $T \approx 1.5T_f$). The magnetization can be expressed as

$$M \approx m_0 + \chi_0 H - b_3(\chi_0 H)^3 + b_5(\chi_0 H)^5 + \dots$$

The constant term accounts for a possible remanent magnetization in the superconducting magnet and/or the sample. A least-squares fit of the isothermal magnetization curves constructed from our field-cooled data to the above expression yields values for χ_0 , b_3 and b_5 .

Figures 8–10 show the temperature dependence of b_3 and b_5 obtained from these fit, for samples $x = 0.7, 1$, and 1.7 . A more detailed analysis of the possibility of critical behavior close to T_f is out of the scope of this paper, but an inspection of these plots confirms the relevance of the non-linear contributions to the magnetization developing on

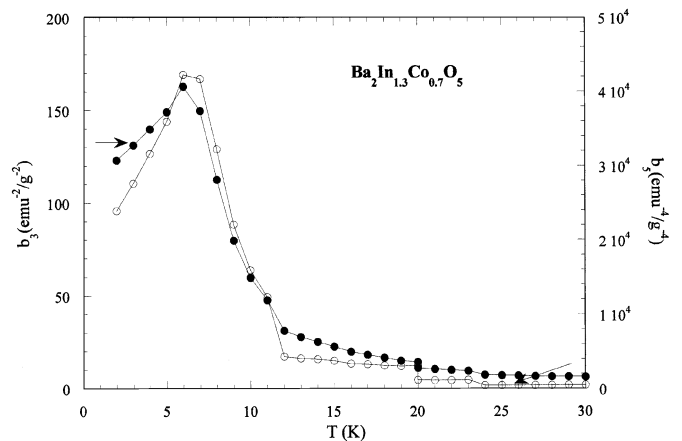


FIG. 8. Thermal variation of the first (b_3) and second (b_5) nonlinear susceptibility coefficients for $\text{Ba}_2\text{In}_{1.3}\text{Co}_{0.7}\text{O}_5$ oxide.

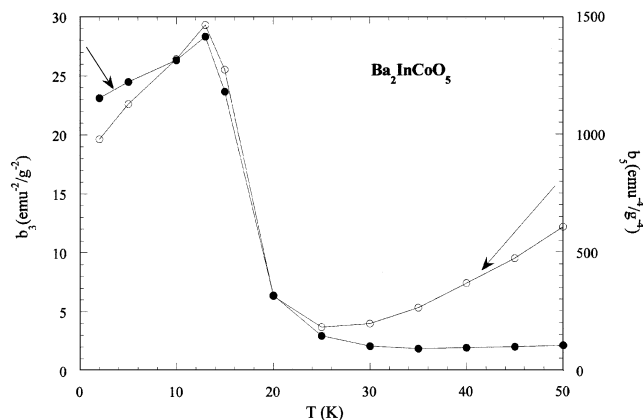


FIG. 9. Thermal variation of the first (b_3) and second (b_5) nonlinear susceptibility coefficients for $\text{Ba}_2\text{InCoO}_5$ oxide.

approaching the freezing temperature, the expected behavior for a spin glass in the frame of mean-field theories. Focusing on b_3 , more representative than b_5 because it was determined more accurately, it shows an increase by a factor of about 30 when between $T=2T_f$ and T_f for samples $x=0.7$ and 1.0. We interpret the maxima in the nonlinear coefficients as the actual freezing temperatures, in full agreement with those determined from the irreversibility observed between the ZFC and FC curves (see figures above). For the sample $x=1.7$, a much less marked increase in b_3 , which amounts to a factor of only 4, was observed. Notice that, compared with the other samples, this one displays broad peaks and smoother features in the ZFC-FC magnetization curves, in agreement with a poorer definition of the freezing temperature revealed by the weak increase of the nonlinear coefficients. Some sample inhomogeneity and/or Co clustering could be expected for these high-Co-content samples very close to the

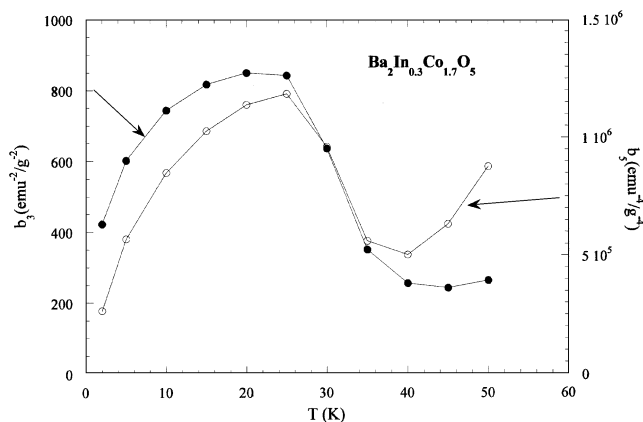


FIG. 10. Thermal variation of the first (b_3) and second (b_5) nonlinear susceptibility coefficients for $\text{Ba}_2\text{In}_{0.3}\text{Co}_{1.7}\text{O}_5$ oxide.

stability limit for its crystallographic structure, as was discussed above.

These results, together with those of ac susceptibility measurements, support the existence in these oxides of a collective magnetic state below T_f , very likely a spin-glass state, at least for samples $x=0.7$ and 1.0. The substantial increase in the nonlinear coefficients that takes place at T_f , although smaller than the 2–3 orders of magnitude typical of canonical spin glasses (34), is completely at variance with the temperature-independent coefficients expected for independent or moderately interacting superparamagnetic grains or clusters (35, 36), the most obvious alternative to spin-glass behavior. We point out that the determination of nonlinear coefficients from M vs H curves is quite often troublesome, due to the difficulty of accurate M (H) measurements at low field when the magnetic moment is low and/or there is some remanent magnetization coming from small amounts of ferromagnetic contaminants. If the spin-glass state displayed by this oxide is similar to that observed in canonical systems or, as the moderate increase in b_3 could lead one to speculate, is related to that observed in other frustrated oxide systems, such as the kagome system $\text{SrCr}_8\text{Ga}_9\text{O}_{19}$ (37), is a question that remains open for further research.

CONCLUSIONS

Magnetic measurements, discussed in detail above, confirm the spin-glass behavior of the oxides of general formula $\text{Ba}_2\text{In}_{2-x}\text{Co}_x\text{O}_5$ ($x=0.70, 1, 1.70$). The origin of this spin-glass behavior could be due to different reasons:

(i) Chemical site disorder, as has been demonstrated from X-ray diffraction studies, which should contribute to the frustrated magnetic ground state.

(ii) The presence simultaneously of Co^{3+} as high spin (HS) and intermediate spin (IS) give rise to the competition of ferro- and antiferromagnetic interactions, yielding magnetic frustration. This frustration could have its origin in the competing ferromagnetic and antiferromagnetic interactions between the nearest neighbors and the next nearest neighbors, which are intrinsic in a cubic arrangement. Similar results have been recently reported in a completely disordered perovskites (16, 17).

ACKNOWLEDGMENTS

We thank DGICYT for financial support, under Projects MAT-2000-0753-C02-01 and 1FD97-1422MAT from EU-CICYT.

REFERENCES

1. J. B. Goodenough, J. E. Ruiz Diaz, and Y. S. Zhen, *Solid State Ionics* **44**, 21 (1990).
2. D. H. Gregory and M. T. Weller, *J. Solid State Chem.* **107**, 134 (1993).
3. F. R. Cruickshank, D. Mck. Taylor, and F. P. Glasser, *J. Inorg. Nucl. Chem.* **26**, 937 (1964).

4. L. M. Kovba, L. N. Lykova, and T. A. Kalinina, *Russ. J. Inorg. Chem.* **25**, 397 (1980).
5. T. A. Kalinina, L. N. Lykova, M. G. Melnikova, and N. V. Porotnikov, *Russ. J. Inorg. Chem.* **28**, 259 (1983).
6. K. Mader and H. K. Muller-Buschbaum, *Z. Anorg. Allg. Chem.* **559**, 89 (1988).
7. K. Mader and H. K. Muller-Buschbaum, *Z. Anorg. Allg. Chem.* **573**, 12 (1989).
8. R. V. Schenck and H. K. Muller-Buschbaum, *Z. Anorg. Allg. Chem.* **395**, 280 (1973).
9. A. A. Colville and S. Geller, *Acta Crystallogr. Sect. B* **27**, 2311 (1971).
10. A. L. Kharlanov, N. R. Khasanova, M. V. Paromova, E. V. Antipov, L. N. Lykova, and I. M. Kovba, *Russ. J. Inorg. Chem.* **35**, 1741 (1990).
11. I. Julián Ortega, R. Sáez Puche, J. Romero de Paz, and J. L. Martínez, *J. Mater. Chem.* **9**, 525 (1999).
12. X. Obradors, A. Labarta, A. Isalgué, J. Tejada, J. Rodríguez Calvajal, and M. Pernet, *Solid State Commun.* **65**, 189 (1988).
13. A. P. Ramirez, R. Jager-Waldan, and T. Siegrist, *Phys. Rev. B* **43**, 10461 (1991).
14. R. J. Cava, A. P. Ramirez, Q. Huang, and J. J. Krajewski, *J. Solid State Chem.* **140**, 337 (1998).
15. A. Maignan, B. Raveau, C. Martin, and M. Hervieu, *J. Solid State Chem.* **144**, 224 (1999).
16. K. Yoshii, *J. Solid State Chem.* **151**, 294 (2000).
17. V. Primo-Martin and M. Jansen, *J. Solid State Chem.* **157**, 76 (2001).
18. M. Itoh, M. Mori, S. Yamaguchi, and Y. Tokura, *Physica B* **259–261**, 902 (1999).
19. K. Asai, A. Yoneda, O. Yokokura, J. M. Tranquada, G. Shirane, and K. Hohn, *J. Phys. Soc. Jpn.* **67**, 290 (1998).
20. H. M. Rietveld, *J. Appl. Crystallogr.* **2**, 65 (1969).
21. J. Rodríguez-Carvajal, "Guide of Fullprof." Laboratoire Léon Brillouin, Saclay, 1998.
22. H. Taguchi, Y. Takeda, F. Kanamaru, M. Shimada, and M. Koizumi, *Acta Crystallogr. Sect. B* **33**, 1298 (1977).
23. B. E. Gushee, L. Katz, and R. Ward, *J. Amer. Chem. Soc.* **79**, 5601 (1957).
24. B. N. Figgis and M. A. Hitchman, "Ligand Field Theory and its Applications." Wiley VCH, New York, 2000.
25. P. M. Raccach and J. B. Goodenough, *Phys. Rev.* **155**, 932 (1967).
26. B. Buffat, G. Demazeau, M. Pouchard, and P. Hagenmuller, *Proc. Indian Acad. Sci.* **93**, 313 (1984).
27. M. A. Señaris Rodríguez and J. B. Goodenough, *J. Solid State Chem.* **116**, 224 (1995).
28. M. Itoh, I. Natori, S. Kubota, and K. Motoya, *J. Phys. Soc. Jpn.* **63**, 1486 (1994).
29. J. A. Mydosh, "Spin Glasses: An Experimental Introduction" Taylor & Francis, London, 1993.
30. J. R. Almeida and D. J. Thouless, *J. Phys. A* **11**, 983 (1978).
31. J. J. Prejean and J. Souletie, *J. Phys. (Paris)* **41**, 1335 (1980).
32. L. Neel, *C. R. Hebd. Seances Acad. Sci.* **252**, 4075 (1961).
33. S. Kirkpatrick and D. Sherrington, *Phys. Rev. Lett.* **35**, 1972 (1975); *Phys. Rev. B* **17**, 4384 (1978).
34. R. Omari, J. J. Prejean, and J. Souletie, *J. Phys. (Paris)* **44**, 1069 (1983).
35. D. Fiorani, J. Tholence and J. L. Dormann, *J. Phys. C* **19**, 5495 (1986).
36. J. A. De Toro, M. A. López de la Torre, J. M. Riveiro, R. Sáez-Puche, A. Gómez-Herrero, and L. C. Otero-Díaz, *Phys. Rev. B* **60**, 12918 (1999).
37. B. Martínez, A. Labarta, R. Rodríguez-Solá, and X. Obradors, *Phys. Rev B* **50**, 15779 (1994).